

## $\lambda$ -DNA Induced Turbulent Drag Reduction and Its Characteristics

S. T. Lim and H. J. Choi\*

*Department of Polymer Science and Engineering, Inha University, Incheon, 402-751, Korea*

S. Y. Lee and J. S. So

*Department of Biological Engineering and Center for Advanced Bioseparation Technology, Inha University, Incheon, 402-751, Korea*

C. K. Chan

*Institute of Physics, Academia Sinica, Taipei, Taiwan, 115, Republic of China*

*Received December 15, 2002; Revised Manuscript Received May 19, 2003*

**ABSTRACT:** Turbulent drag reduction (DR) induced by monodispersed high molecular weight  $\lambda$ -DNA in a buffer solution under a turbulent flow was investigated using a rotating disk apparatus. The DR efficiency was maintained over time due to the durability of the  $\lambda$ -DNA in a moderate turbulent shear flow, and this behavior was compared to a water-soluble linear flexible long chain polyacrylamide (PAAM). To investigate the mechanical degradation mechanism of  $\lambda$ -DNA, the maximum drag reducing rotation speed (rpm) of the disk was examined by increasing the rotation speed using two different modes to increase the rpm: a continuous and stepwise mode. The mechanical degradation of  $\lambda$ -DNA with a high turbulent flow was analyzed using an electrophoresis method, which indicated a midpoint scission of the long chain molecules. The DR efficiency at different rotation speeds and results of a long-term experiment also supported the half-length degradation of  $\lambda$ -DNA and strong resistance of the helically stranded  $\lambda$ -DNA structure in a turbulent flow compared to its water-soluble flexible counterpart.

### Introduction

Under certain conditions of turbulent flow, the drag friction of a dilute polymer solution is drastically reduced by even minute amounts of suitable additives, implying that polymer solutions undergoing flow in a pipe require a lower pressure gradient to maintain the same flow rate. This phenomenon has already been extensively investigated not only for its wide range of applications<sup>1–3</sup> but also for its scientific interest,<sup>4–6</sup> and several parameters, including the polymer concentration, polymer molecular weight, temperature, Reynolds number, and solvent quality, have already been identified as important factors.<sup>1</sup>

Among the various drag-reducing polymers, high molecular weight polymers with a linear flexible structure, such as water-soluble poly(ethylene oxide) (PEO),<sup>7</sup> poly(acrylamide) (PAAM), and oil-soluble polyisobutylene (PIB),<sup>7,8</sup> have been particularly examined. While both PEO and PAAM are generally accepted as drag reducers in aqueous systems, PIB in organic solvents is known to exhibit a low stability against mechanical degradation; thus, it degrades rapidly with time. To reduce the polymer susceptibility to bond scission, commercial biopolymers, such as polysaccharides, have been adopted as drag-reducing agents.<sup>9</sup> The high resistance to turbulent flow of such biopolymers may be associated with their molecular structures. In addition, cationic surfactant systems<sup>10</sup> have also been tested in circulating systems.

In the current study,  $\lambda$ -DNA possessing a relatively higher molecular weight (48 502 base pair, 32 300 kDa) than conventional synthetic polymers was examined as a potential drag-reducing agent in a turbulent flow.

Since  $\lambda$ -DNA has a different molecular structure (helical structure) compared to conventional flexible polymeric drag reducers (usually linear structure), it was anticipated that this configurational structure of  $\lambda$ -DNA would exhibit its own unique behavior in a turbulent flow, thereby providing a more detailed understanding about the drag-reducing phenomenon. When Hand and Williams<sup>11</sup> measured the drag reduction of calf-thymus DNA as a function of the pH, they observed that a less flexible helical conformation was preferable to a random coil for maximum drag reduction. Recently, the current authors also reported that double-stranded DNA was a good drag reducer when compared with linear flexible polymers, such as PEO.<sup>12</sup> Although the mechanism of DR has been the subject of extensive research, it is reasonable to say that its basic mechanism still eludes fundamental and general explanations.<sup>12–15</sup>

Among the various efforts to explain the DR phenomena along mechanical degradation in a flow, Brostow<sup>16</sup> developed a statistical-mechanical model of polymer chain conformation and further showed ultrasonically determined solvation numbers for a series of copolymers with the same chemical structure yet differing widely in their intrinsic viscosities. These experimental results were found to correlate well with the theory<sup>2</sup> that explains DR in dilute polymer solutions in terms of the solvation of macromolecular chains and formation of relatively stable, energy-sinking domains.

Conversely, an elastic theory of DR was also introduced to discuss the properties of homogeneous, isotropic three-dimensional turbulence in the presence of polymer additives without any wall effect.<sup>17,18</sup> The central idea of this “cascade theory”, limited to linear flexible chains in a good solvent, is that small scale polymer effects are not determined by the viscosity but rather by the elastic modulus. The importance of an elastic property in determining the mechanism of drag

\* Corresponding author: Tel +82-32-860-7486; fax +82-32-865-5178; e-mail hjchoi@inha.ac.kr.

reduction was also examined by Armstrong and Jhon.<sup>19</sup> Adopting a simple model to study both the turbulence and dissolved polymer molecules, they related the molecular dissipation with friction factors by constructing a self-consistent method and found that a polymer molecule grows by a factor of 10 or more from its equilibrium conformation.

Meanwhile, in a turbulent flow, polymer additives are exposed to high elongational strain as well as high shear, which can lead to the scission of polymer chains. Consequently, the DR effectiveness decreases with the elapsed time.<sup>20,21</sup> This mechanical molecular degradation in a turbulent flow is also related to various factors, such as the polymer molecular weight distribution (MWD), solution temperature, polymer-solvent pairing, polymer concentration, turbulent intensity, and flow geometry.<sup>22-24</sup>

Several theories have conjectured that the extreme extension of polymer chains causes the polymer molecules to undergo mechanical degradation.<sup>25</sup> In addition, polymer degradation is also closely related to the polymer-solvent interaction. Therefore, when combining these two concepts, it can be intuitively claimed that polymer molecules may degrade more rapidly in a good solvent, in which the polymer chains are more vulnerable to extension under flow. However, contrary to this argument, Moussa et al.<sup>26</sup> found that polymer molecules degraded more rapidly in poor solvents at low Reynolds numbers, while an opposite trend occurred at high Reynolds numbers, suggesting that this difference was due to the existence of two possible mechanisms of polymer stretching and intramolecular entanglements. Brostow<sup>16</sup> also reported that more mechanical degradation was observed in a poor solvent than in good solvents under the same flow conditions.

There are several reasons why  $\lambda$ -DNA was selected for the current study. First,  $\lambda$ -DNA possesses a relatively high molecular weight with a perfect monodispersity, which is not easy to obtain with a synthetic polymer. In addition, its molecular weight can be accurately characterized using electrophoresis due to its intrinsic electrically negative charge. As such,  $\lambda$ -DNA can be considered as a model polymer and has been extensively used recently.<sup>27-32</sup> Second, the length of a fully stretched  $\lambda$ -DNA is comparable to the microscales of a turbulent flow. Since the lengths of the polymers traditionally used in DR studies are much smaller than the microscales of the turbulence, the interaction between the polymer and the flow can be quite different. Finally, a significant change in the molecular properties of  $\lambda$ -DNA can be induced by a change in pH or temperature. At the appropriate pH or temperature, the  $\lambda$ -DNA molecule changes from its double-strand (ds) natural state to a denatured state of two single-strand (ss) molecules. Therefore, this configurational change may help to probe the details of the DR phenomenon.<sup>12</sup>

## Experimental Section

**Materials.** A  $\lambda$ -DNA sample, acquired from the Promega Corp. (US), that was 48 502 bp (32 300 kDa) in size was used, in which the  $\lambda$ -DNA c1857 Sam 7 was isolated from an infected *Escherichia coli* strain, W3350, that is commonly used as a substrate in a restriction enzyme activity assay. Prior to the drag reduction experiment, the  $\lambda$ -DNA was stored at  $-20^\circ\text{C}$ . The DR measurement was performed in a buffer solution for  $\lambda$ -DNA, which consisted of 10 mM Tris-HCl, 10 mM NaCl, and 1 mM EDTA. The buffer solution (pH 7.8 at  $25^\circ\text{C}$ ) was chosen because it preserved the double-stranded helical structure of  $\lambda$ -DNA.

In general, most effective conventional drag-reducing polymers possess a linear flexible structure and very high molecular weight. Among these, a high molecular weight water-soluble polyacrylamide (PAAM,  $M_w$   $1.8 \times 10^7$ , Polyscience Inc., Warrington, PA) was selected as a comparison for the drag-reducing behavior of  $\lambda$ -DNA. The DR test for this water-soluble polymer was performed in distilled water.

**Apparatus and Measurements.** A rotating disk apparatus (RDA) was used to study both the DR efficiency and the transient behavior of the  $\lambda$ -DNA chains as a function of time in a turbulent flow. The specifications of the RDA have been previously reported.<sup>33</sup> The device consisted of an aluminum disk, 14.5 cm in diameter and 0.32 cm thick, enclosed in a cylindrical, temperature-controlled container composed of aluminum with an inner diameter of 16.3 cm and height of 5.5 cm. An electric transducer was used to monitor the torque exerted on the disk rotating at a specific speed. (It also determined the Reynolds number,  $N_{Re}$ , in conjunction with other experimental conditions.)

Note that the phenomenon of DR has not been studied in external flows as extensively as in pipe flows.<sup>7,25,35-39</sup> Therefore, since drag reduction is known to be related only to the friction drag, the current study adopted a rotating disk system to describe the external flow, including the flow over flat plates, as well as the flow around submerged objects and the Couette flow.<sup>34</sup> One studies typical friction drag for an internal flow, whereas the other studies the total drag (friction plus form drag) for an external flow. The drag reduction is known to be related only to the friction drag. Therefore, to study the total drag reduction, the rotating disk system has been adopted.<sup>7,25,35-39</sup>

The turbulence was produced according to the rotational Reynolds number ( $N_{Re}$ )  $> 3 \times 10^5$  or, equivalently, the rotational speed of the disk ( $\omega$ )  $> 570$  rpm. Here,  $N_{Re} \equiv \rho r^2 \omega / \mu$ , where  $\rho$  is the fluid density,  $\mu$  is the fluid viscosity, and  $r$  is the radius of the disk. The temperature of the system was maintained at  $25 \pm 0.5^\circ\text{C}$  during the tests.

At first, the RDA reservoir was filled with 370 mL of the buffer solution, and then the temperature was adjusted to  $25^\circ\text{C}$ . The  $\lambda$ -DNA in a frozen state was melted and injected into the turbulent flow field using a micropipet. For the DR measurement, 515  $\mu\text{g/mL}$  of the DNA stock solution was used. The %DR was then obtained as a function of time by injecting measured quantities of the stock solution directly into the turbulent flow field generated by the RDA. The torque required to rotate the disk with the pure solvent ( $T_s$ ) at a given speed was measured first. The percent DR (%DR) was then calculated by measuring the corresponding torque required with the dilute polymer solution ( $T_p$ ) at the same  $\omega$  as follows:

$$\%DR = \frac{T_s - T_p}{T_s} \times 100 \quad (\text{at a given } N_{Re}) \quad (1)$$

Furthermore, an electrophoresis analysis was used to examine the mechanical degradation of the  $\lambda$ -DNA by measuring the size of its base pair (bp) using a sample that had been exposed one time to the turbulent flow.

## Results and Discussion

Figure 1 shows the %DR of  $\lambda$ -DNA for three different  $\lambda$ -DNA concentrations at 1.35, 2.30, and 2.70 wppm as a function of time at a relatively high Reynolds number ( $N_{Re} \sim 1\,000\,000$ ), where such a high turbulence was generated by a high disk rotation speed ( $\sim 1980$  rpm). Despite the low concentrations of  $\lambda$ -DNA used in the current study, a relatively high drag-reducing efficiency was produced that increased with the  $\lambda$ -DNA concentration. However, the %DR efficiency decreased with time due to the mechanical degradation of  $\lambda$ -DNA. Although  $\lambda$ -DNA was degraded in a high turbulent flow, the %DR efficiency was still maintained for a long time after an initial drop. This behavior is significantly different from that of other kinds of drag-reducing polymers with

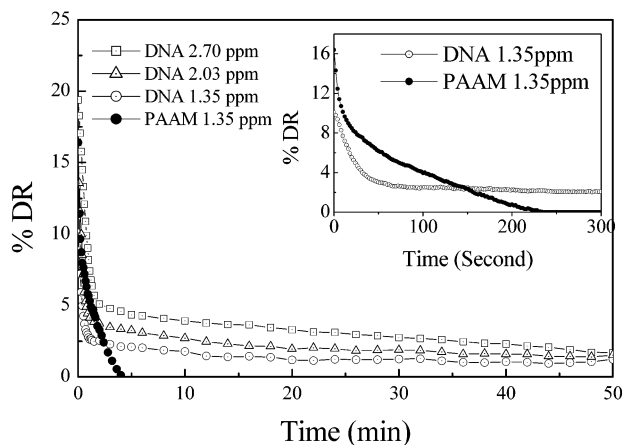


**Figure 1.** Comparison of  $\lambda$ -DNA percent drag reduction (1.35, 2.03, and 2.70 wppm) with PAAM ( $M_w = 18 \times 10^6$  g/mol) on long-term scale (1 h) at 1980 rpm ( $N_{Re} = 1 \times 10^6$ ) and 25 °C. The inset represents the initial changes in the drag reducing efficiency for  $\lambda$ -DNA and PAAM at 1.35 wppm.

linearly long chain molecules, as flexible long chain molecules are known to degrade as soon as they are injected into a high turbulent flow.<sup>16,24,40</sup> The durability of  $\lambda$ -DNA to high turbulence was assumed to originate from its very strong helical structure under proper conditions. Thus, to examine the long-term behavior of  $\lambda$ -DNA in a turbulent flow, the turbulent experimental conditions were maintained for 1 h.

A drag reduction experiment was also conducted with a linear flexible polymer (PAAM) to compare its long-term durability with that of  $\lambda$ -DNA (Figure 1). In the case of  $\lambda$ -DNA, it degraded within a few minutes of the initial injection; thereafter, when the %DR reached a limiting value, the resulting %DR efficiency was maintained for a long time. Meanwhile, the DR efficiency of PAAM decreased abruptly within a few minutes, and no further DR efficiency was observed. Although  $\lambda$ -DNA also exhibited a continuous decrease under the same conditions as PAAM, the slope of decrease was lower than that for PAAM within a few seconds, and a limited DR efficiency maintained, as shown in the inset in Figure 1. Another interesting feature was that  $\lambda$ -DNA always displayed nearly the same limiting value, indicating possible evidence of a midpoint degradation of the  $\lambda$ -DNA molecule. Various researchers<sup>24,40</sup> have proposed a degradation mechanism for long chain molecules in a turbulent flow and showed that the degradation usually occurs at the midpoint based on the polydispersity index of the polymer. Therefore, in the current study, the residual maintenance of the drag-reducing efficiency was thought to originate from the strong endurance of the  $\lambda$ -DNA molecule in turbulence, indicating that even though the  $\lambda$ -DNA molecules underwent a degradation process in high turbulence, residual short chain molecules that were not degraded under such conditions remained as a drag reducer. As such, when compared with PAAM, the DR efficiency of  $\lambda$ -DNA was still effective even in a very strong turbulent flow. The molecular weight change of  $\lambda$ -DNA induced from the DR experiment was confirmed using an electrophoresis method, and the results are discussed later on. To examine the initial decrease of drag reducing efficiency, the results for the initial time period were magnified. The inset in Figure 1 shows the main difference between the decreasing behavior of  $\lambda$ -DNA and that of PAAM. The slope of the drag reduction for

$\lambda$ -DNA was less steep than that for PAAM. In other words, the relative decrease of the DR effect for PAAM was more severe than that for  $\lambda$ -DNA within about 30 s. In the case of PAAM, the decreasing behavior continued until its %DR became zero. Usually, long flexible chain molecules, such as PAAM, possess a polydispersity with a molecular weight distribution (MWD). Thus, if it is assumed that long chain polymers experience midpoint degradation, polymer chains with different molecular weights should show a different time-dependent resistance. For example, longer molecules will be more susceptible to mechanical degradation, accompanied by more rapid degradation. This mechanism could explain the difference in the initial slope for the %DR and continuous decrease of DR efficiency with time for the PAAM system.

Furthermore, in the current study, it was also observed that the degradation slopes of DR efficiency were almost the same, regardless of different concentrations under the same turbulent conditions (Reynolds number  $> 10^6$ ).<sup>12</sup> However, the asymptote value for each concentration increased with the concentration of  $\lambda$ -DNA, indicating that although there were some differences in the initial DR efficiency, the overall degradation mechanism was the same under all the different conditions. As such, the concentration difference only affected the time taken to reach the asymptote DR value. This result also supports the midpoint scission of  $\lambda$ -DNA under high turbulent conditions, as an increase in the concentration only gave rise to an increase in the half-length DNA quantity. This could also explain why there was no further development of the degradation process in this condition. As far as concerned on this half-cut phenomenon, Sasaki et al.<sup>41</sup> explained it within a theoretical framework known as the thermally activated barrier to scission (TABS) model.<sup>42</sup> According to this model, molecular degradation in an elongational flow field proceeds in two-stage processes: molecular stretching and fracture. In this process, scission of the extended conformation always occurs near the midpoint, where the stress in the molecule reaches a maximum value, in accordance with the theoretical prediction of Frenkel.<sup>43</sup> Regarding the critical condition of molecular degradation, Sasaki et al.<sup>41</sup> also explained that the critical strain rate ( $\dot{\epsilon}_f$ ) for fracture is related to the contour length ( $L$ ) and then to the molecular weight ( $M_w$ ) of a polymer chain in an inverse square mode:<sup>43</sup>  $\dot{\epsilon}_f \propto 1/L^2 = 1/M_w^2$ . This indicates that a polymer chain, experiencing mechanical degradation, needs a higher strain rate for its next-step scission. In a sufficiently strong turbulent flow, the multistep degradation process can occur. Nonetheless, this model strongly supports the single step half-cut degradation process of  $\lambda$ -DNA in this study, if the critical strain rate for half-cut  $\lambda$ -DNA is much higher than the flow field.

Linear long chain molecules usually exhibit a maximum drag efficiency at a specific temperature, polymer concentration, and rotation speed. Thus, to examine the maximum drag-reducing conditions, two types of rotation speed sweep test were conducted. At a given specific temperature (25 °C) and concentration (1.35 wppm), the speed of the rotating disk was increased in either a continuous or stepwise mode. Each mode of increasing the speed provided different information on  $\lambda$ -DNA behavior in a turbulent flow. Figure 2 shows the variation in the shaft torque with a continuous increase in the rotation speed, and a maximum value was exhibited at a specific rotation speed. When these



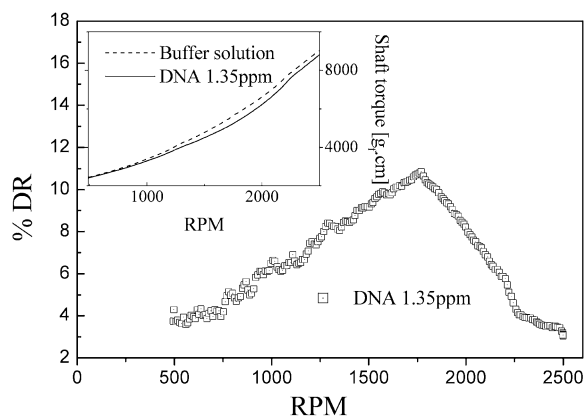


**Figure 2.** Percent drag reduction vs rpm ( $N_{Re} = 2.5 \times 10^5$ – $1.3 \times 10^6$ ) for 1.35 wppm  $\lambda$ -DNA in buffer solution at 25 °C (continuous mode rpm sweep). The inset shows the shaft torque variation with the continuous rpm sweep mode (sweep rate 20 rpm/s).

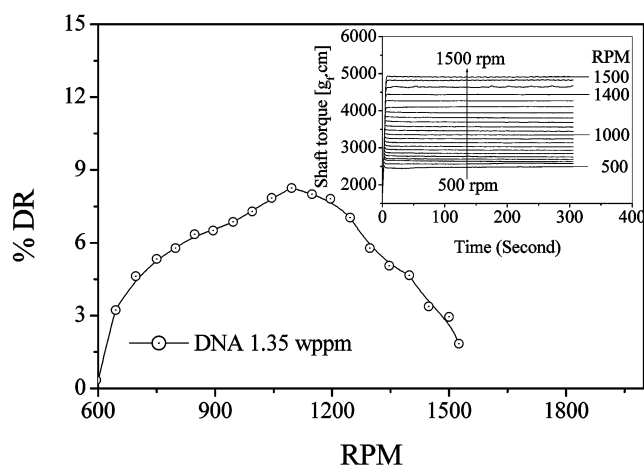


**Figure 3.** Percent drag reduction vs rpm ( $N_{Re} = 2.5 \times 10^5$ – $7.7 \times 10^5$ ) for 1.35 wppm  $\lambda$ -DNA in buffer solution at 25 °C (stepwise mode rpm sweep). The inset shows the shaft torque for a 1.35 wppm solution of  $\lambda$ -DNA with the stepwise mode rpm sweep (500–1500 rpm) at 25 °C (interval; 300 s, 50 rpm/step).

results were replotted to determine the DR efficiency as a function of the rpm, the optimal conditions were easily designated as the peak position of the %DR curve, where the maximum drag efficiency of 11% occurred at 1770 rpm, corresponding to a Reynolds number of 908 000 (see Figure 2). Usually, the DR phenomenon caused by a polymeric additive is more effective in a higher turbulent flow, until a critical condition is reached. Beyond this critical condition, polymer chains may experience more severe (apparent) degradation due to the excess energy generated by the turbulent flow. This result will be further discussed in conjunction with the results of separate DR experiments at different rotation speeds (Figure 5) (1400–2350 rpm). In the case of Figure 1, the experimental conditions (i.e., rotation speed) were already above the critical point, which is why the initial %DR value proceeded to a degradation process with time. When comparing Figures 1 and 2, the initial %DR (11%) in Figure 1 (1.35 and 1980 rpm) was higher than that (8%) obtained at the same rotation speed with a continuous rpm sweep mode (Figure 2). This was due to the fact that, with the continuous mode, the degradation continued until the rpm reached a strong turbulent condition (1980 rpm). In the current experiment, the rotation speed was increased at a rate

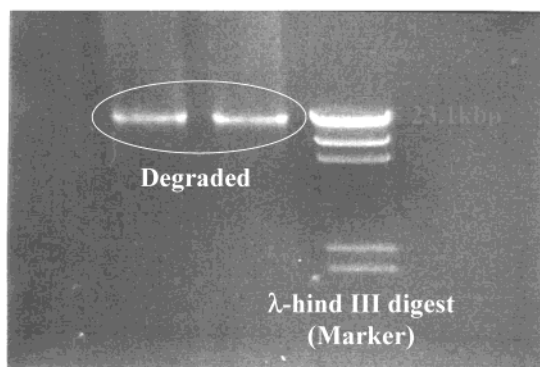


**Figure 4.** Electrophoresis results for  $\lambda$ -DNA after degradation under turbulent flow for 1 h at 1980 rpm and 25 °C.

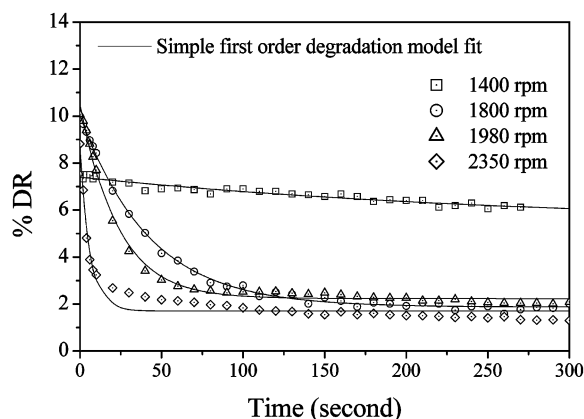


**Figure 5.** Drag reduction efficiency as a function of time for 1.35 wppm of  $\lambda$ -DNA in buffer solution at different rotation speeds (1400–2350 rpm), 25 °C. Solid line represents values obtained from eq 4, and points represent experimental data.

of 20 rpm/s. As a result, the time taken to reach 1980 rpm with the continuous mode was about 10 s. When examining the %DR 10 s after  $\lambda$ -DNA injection with a fixed rpm test mode, the %DR exhibited almost the same value ( $\sim 8\%$ ) as that with the continuous mode (1980 rpm), indicating that a similar severe molecular degradation process occurred with both test modes (fixed rpm mode and continuously increasing rpm mode) within the same time period. As such, this may explain the differences in the DR efficiencies at a specific rotation speed with different test modes. Plus, the maximum DR efficiency with the continuous rpm sweep test can also help explain the nearly constant %DR with a moderate turbulent flow that was much weaker than the critical condition.

Using the above continuously increasing mode, information was gained about the degradation of  $\lambda$ -DNA in a strong turbulent flow as a function of the rotation speed. However, with such a mode, it is difficult to ascertain the drag-reducing behavior as a time function for each rotation speed. Thus, a stepwise test was performed for each rotation speed, where the rotation speed was maintained for 300 s at each step. The rotation speed was initially set at 500 rpm and increased by 50 rpm in each step. The torque variation for each step is shown in the inset in Figure 3. Although it was difficult to find a distinguishable shaft torque change during the stepwise test, a different result was observed from that in Figure 2 when the results were replotted using the %DR scale. In Figure 3, each %DR value corresponding to a specific rotation speed was represented as a dot-centered circle. For readers' convenience,

in comparison with Figure 2, all data points were connected using a smooth line. The maximum %DR rotation speed and %DR were lower than those with the continuous mode. With the stepwise mode, the maximum %DR speed was obtained at around 1100 rpm, with a %DR of about 8%, indicating the existence of some minor degradation of  $\lambda$ -DNA, even though the rotation speed was below the critical speed of the continuous mode. Since this kind of minor degradation is not common in linear flexible polymer systems, the degradation mechanism of DNA in a turbulent flow would appear to be divided into two types: minor and apparent degradation.

As shown in Figure 3, near the critical rotation speed of the stepwise test mode (1157 rpm), no degradation behavior of  $\lambda$ -DNA was apparent, plus a nearly constant %DR was maintained during the time interval (600 s) when other linear polymers usually exhibit distinct degradation behavior. Furthermore, the %DR saturation value was almost the same as that in the 1400 rpm test (5.1%). Accordingly, this trend of the same saturation value indicates that the minor degradation below the critical rotation speed, from which apparent degradation starts, was not a function of the rotation speed but rather a function of time, which is distinct from the drag-reducing behavior of linear polymers.

The degradation of  $\lambda$ -DNA based on analyzing Figure 1 was also verified using an electrophoresis method. A solution sample taken after the strong turbulent flow DR experiment (1980 rpm,  $N_{Re} \sim 1\,000\,000$ ) was concentrated and then placed in a sample well of agarose gel in an electrophoresis device. Since DNA usually has a negative charge, when the DNA molecules are placed in a well of agarose positioned close to a negative electrode, they migrate toward the positive electrode under an applied electric field, passing through the different sized agarose pores. In Figure 4, the up and down side correspond to the negative and positive electrode, respectively. Prior to the electrophoresis test, the degraded  $\lambda$ -DNA and a reference marker (mixture of precisely cut DNA) were treated with fluorescence dye to identify the position of the DNA after the application of the electric field. The length distribution of the concentrated sample of degraded  $\lambda$ -DNA was analyzed in an electrophoresis device against a sample of known length markers. The length of the degraded DNA was measured by comparing the positions of the electrophoresis bands produced by the length markers. The vertically stacked bars on the right are the positions of the markers, indicating the reference DNA size. The markers were prepared using commercial  $\lambda$ -DNA that had been cut to various exact sizes using a restriction enzyme. The first row was 23.1 kbp (kilobase pair), and the reason why half the 48 kbp DNA appeared as 23.1 kbp instead of 24 kbp was due to the specific sequence of  $\lambda$ -DNA cut by the enzyme knife. The size of the  $\lambda$ -DNA after degradation in a turbulent flow found to be was 23.1 kbp. Thus, when compared to the original  $\lambda$ -DNA with a 48 kbp structure, this implies two important results. First,  $\lambda$ -DNA with a monodispersed molecular weight experienced midpoint degradation, thereby confirming the previous theory that the overall degradation of a polymer mainly occurs at the half position of the polymer, where the stress in the molecule reaches a maximum value.<sup>41</sup> In the case of linear flexible polymers, this mechanical degradation behavior has usually been explained on the basis of molecular weight distribution data from gel permeation chromatography (GPC).

Second, the 23.1 kbp size of DNA after degraded still exhibited a very strong resistance to turbulence, which is a somewhat different drag-reducing behavior from linear flexible polymers. This kind of half-cut result of drag-reducing polymeric additives has already been proposed and examined by several investigators,<sup>42,44,45</sup> who demonstrated that an extensional flow-induced chain scission occurs within a fairly narrow distribution around the chain midpoint, indicating that the polymer chains are highly extended when they break. Merrill and Horn<sup>45</sup> also reported on a midpoint scission of macromolecules in a turbulent flow, thereby implying that polymer chains can indeed be fully extended in a turbulent flow as well as in a laminar extensional flow. This hypothesis concurs with various drag reduction theories, which hold that drag reduction is caused by the suppression of extensional portions of the turbulent flow due to an increase in the extensional viscosity. This argument is also consistent with the inverse dependency of the degree of degradation on the polymer concentration.

As explained, certain crucial parameters must be considered to obtain the desired DR efficiency when using linear polymeric drag reducers, such as the concentration of the additive, molecular weight, method of preparation and storage, and flow geometry and rate. However, industrial applications of drag reducers have been hampered by the degradation of the polymers. Among the above-mentioned parameters, the current study examined the drag-reducing behavior with different flow rates (rotation speeds; 1400–2350 rpm) to check the basic relation between rotation speed and  $\lambda$ -DNA degradation. Figure 5 represents the time evolution of the DR efficiency at various rotation speeds. For fixed rotation speeds of 1400, 1800, 1980, and 2350 rpm, the resulting DR efficiency was 7.51, 9.91, 10.1, and 8.82%, respectively. The overall trend above the critical rotation speed (1770 rpm with continuous increasing mode) was a distinct decrease in the DR efficiency. Plus, the asymptote values were different for each rotation speed within a short time scale ( $<300$  s), indicating a similar degradation mechanism above the critical degradation condition, as shown in Figure 2. In the case of 1400 rpm, no distinct decrease in the DR efficiency was observed within the initial rotation period. Thus, the rotation speeds were divided into two different regions: minor degradation region and distinct degradation region below and above a critical rotation speed, respectively.

On the basis of the results of the DR experiment at various rotation speeds, a numerical fitting was also conducted using the simple first-order degradation model.<sup>12</sup> If the characteristic degradation of  $\lambda$ -DNA in a turbulent flow is considered to be a midpoint scission, the degradation can be expressed as a function of the molecular length scale ( $L$ ) and half-length ( $L/2$ ), i.e., the size of the degraded  $\lambda$ -DNA. As such, the degradation of  $\lambda$ -DNA, in which the length of  $\lambda$ -DNA ( $L$ ) becomes  $L/2$ , can be described as a first-order reaction with  $\alpha$  as the rate. Here, the number of  $\lambda$ -DNA with length  $L$  at time  $t$ ,  $N_L(t)$ , can be expressed as in eq 2. The mass balance of  $\lambda$ -DNA molecules then leads eq 3.

$$\frac{dN_L}{dt} = -\alpha N_L \quad (2)$$

$$\frac{N_{L/2}(t)}{2} + N_L(t) = N_L(0) \quad (3)$$

**Table 1. Results of Initial Stage Data Fitting for  $\lambda$ -DNA in Buffer Solution at Different Rotation Speeds Using Simple First-Order Degradation Model (Eq 4).**

	rpm			
	1400	1800	1980	2350
$w_1$	31.6	11.7	12.0	10.6
$w_2$	29.6	3.55	3.72	3.53
$\alpha$	0.003	0.024	0.044	0.173
$c$	-24.24	-1.67	-1.48	-1.83
$w_1/w_2$	1.07	3.34	3.24	3.02

As a result, the degradation features at different rotation speeds can be fitted and numerically expressed by the coefficients in eq 4 as a first-order approximation where  $w(L)$  is the drag reducing power dependence on  $L$  and  $c$  is the background contribution due to systematic uncertainties in the measurement.

$$\begin{aligned}\%DR(t) &= w(L) N_L(t) + w(L/2) N_{L/2}(t) + c \\ &= w_1 e^{-\alpha t} + w_2 (1 - e^{-\alpha t}) + c\end{aligned}\quad (4)$$

Using this equation, the physical interpretation of the DR and mechanical molecular degradation can be described using two time-independent parameters,  $\alpha$  and  $w$ . The solid lines in Figure 5 are obtained from nonlinear curve fitting for  $\alpha$  and  $w$  using the simple first-order degradation model. The results are summarized in Table 1. Although the fitted line for 2350 rpm showed a minor deviation from the experimental results, it was still regarded as acceptable when considering the overall degradation features for different turbulent conditions, as shown in Table 1. Therefore, the effect of the turbulent strength on the degradation of  $\lambda$ -DNA was determined on the basis of the resulting parameters of  $\alpha$  and  $w$ . As shown in Table 1, the rate constant ( $\alpha$ ) increased with the rotation speed. In particular, the results from the 1400 rpm test were much lower than those from the other higher rpm cases in the order of magnitude, indicating that the degradation procedure was quite different and less severe under the mild degradation conditions with a lower rotation speed, as seen in Figure 5. Similar to this result,  $w_1$ , the drag-reducing power dependence on  $L$  was distinctly different for the higher rpm cases. The value ( $w_1 = 31.6$ ) for 1400 rpm was much larger than that for the higher rpm cases (1800, 1980, and 2350 rpm). Except for the 1400 rpm case, the values had a similar magnitude with a slightly increasing trend according to the turbulent strength. This is also further evidence of a quite different decrease in the DR efficiency between extremely high rotation speed conditions (1800, 1980, and 2350 rpm) and mild degradation ones (1400 rpm).

Ideally, the fitting ratio  $w(L)/w(L/2)$  should be the same at a fixed concentration (here, 1.35 ppm). Although the drag-reducing power ratio for the 1400 rpm test was almost unity for mild degradation conditions, the values for the other cases were about three, supporting the fact that longer polymers are better drag reducers.<sup>1</sup> The rate constant  $\alpha$  also contains information on the dynamics of degradation. If the turbulence is space filling,  $\alpha$  can be estimated as the inverse of the turn over time for the largest eddy, which is about 0.03 s,<sup>12</sup> suggesting that high-shear regions in a turbulent flow are concentrated in a small fraction of the total volume in the case of 1800 rpm, about  $0.02 \times 0.03 \sim 6 \times 10^{-4}$ , which is about 2 orders of magnitude smaller than the predictions of the current intermittency model.<sup>46</sup> This discrepancy is prob-

ably due to the fact that mechanical molecular degradation requires not only velocity fluctuations with a high shear rate but also a long enough duration so that the molecules are fully stretched. As such, the probability of having both a large and long-life fluctuation would appear to be small.<sup>12</sup>

Conversely, it should also be noted that in an effort to explain the relationship between drag reduction and molecular degradation, Brostow et al.<sup>47</sup> developed the following empirical exponential decay function (with  $h$  as the decay constant):

$$\frac{DR(t)}{DR_0} = \frac{1}{1 + W(1 - e^{-ht})} \quad (5)$$

The DR efficiency and mechanical degradation are related to the macromolecular conformation in the solution, and the DR efficiency is proportional to the molecular weight of the polymers. Thus, this DR efficiency ratio can be considered as the ratio of the effective number-averaged molecular mass at time  $t$  and  $t = 0$  ( $M(t)/M_0$ ). They<sup>47</sup> also noted that the points on the chain where changes of direction occur are more vulnerable to chain scission. Depending on their specific location, some of these points may be protected from degradation by their surroundings, while others will undergo scission under a flow. In the latter case, the average number of points per chain is denoted by  $W$ , which is proportional to the number of breakable sequences with two different orientations, and also can be related to the drag reducer concentration. A larger value of  $h$  indicates fast degradation, while a larger value of  $W$  implies a low shear stability. Detailed comparisons with various different degradation models, including Brostow's model on the molecular degradation of  $\lambda$ -DNA, will be examined in future studies.

In conclusion, the configurational characteristics (double helix) of  $\lambda$ -DNA produced a relatively high drag-reducing effect and resistance to a turbulent flow even at very low concentrations (a few ppm range). With regard to the mechanical degradation of  $\lambda$ -DNA, it exhibited a distinctly different initial and long-term degradation behavior from PAAM. Although  $\lambda$ -DNA degraded more rapidly at first, it reached a constant drag reducing efficiency soon after injection ( $\sim 1$  min). This residual drag-reducing efficiency can be considered as indirect evidence of a midpoint scission of  $\lambda$ -DNA due to the turbulent flow. Meanwhile, the monodisperse molecular weight distribution revealed by an electrophoretic device directly showed that the degraded  $\lambda$ -DNA molecules had been cut in half.

Finally, a simple first-order degradation model was applied to the results of the  $\lambda$ -DNA drag-reducing experiments at various rotation speeds, and the numerically expressed behavior relative to the characteristic parameters fit well with the experimental data. Accordingly, the current results confirm the half-length degradation of  $\lambda$ -DNA and strong resistance of the helically stranded  $\lambda$ -DNA structure in a turbulent flow.

**Acknowledgment.** This study was supported by research grants from the Korea Science and Engineering Foundation (KOSEF) through the Applied Rheology Center (ARC), an official KOSEF-created engineering research center (ERC) at Korea University (Seoul), Korea.



## References and Notes

- (1) Kulicke, W.-M.; Kötter, M.; Gräger, H. *Adv. Polym. Sci.* **1989**, *89*, 1.
- (2) Brostow, W.; Majumdar, S.; Singh, R. P. *Macromol. Rapid Commun.* **1999**, *20*, 144.
- (3) Yoon, S. M.; Kim, N. J.; Kim, C. B.; Hur, B. K. *J. Ind. Eng. Chem.* **2002**, *8*, 564.
- (4) Chertkov, M. *Phys. Rev. Lett.* **2000**, *84*, 4761.
- (5) Sreenivasan, K. R.; White, C. M. *J. Fluid Mech.* **2000**, *409*, 149.
- (6) Govindarajan, R.; L'vov, V. S.; Procaccia, I. *Phys. Rev. Lett.* **2001**, *87*, 17451.
- (7) Choi, H. J.; Jhon, M. S. *Ind. Eng. Chem. Res.* **1996**, *35*, 2993.
- (8) Burger, E. D.; Chorn, L. G.; Perkins, T. K. *J. Rheol.* **1980**, *24*, 603.
- (9) Kim, C. A.; Choi, H. J.; Kim, C. B.; Jhon, M. S. *Macromol. Rapid Commun.* **1998**, *19*, 419.
- (10) Lin, Z. G.; Chou, L. C.; Lu, B.; Zheng, Y.; Davis, H. T.; Scriven, L. E.; Talmon, Y.; Zakin, J. L. *Rheol. Acta* **2000**, *39*, 354.
- (11) Hand, J. H.; Williams, M. C. *Nature (London)* **1970**, *227*, 369.
- (12) Choi, H. J.; Lim, S. T.; Lai, P. K.; Chan, C. K. *Phys. Rev. Lett.* **2002**, *89*, 088302.
- (13) Cressman, J. R.; Bailey, Q.; Goldburg, W. I. *Phys. Fluids* **2001**, *13*, 867.
- (14) Ararouchene, Y.; Kellay, H. *Phys. Rev. Lett.* **2002**, *89*, 104502.
- (15) Stone, P. A.; Waleffe, F.; Graham, M. D. *Phys. Rev. Lett.* **2002**, *89*, 208301.
- (16) Brostow, W. *Polymer* **1983**, *24*, 631.
- (17) Tabor, M.; de Gennes, P. G. *Europhys. Lett.* **1986**, *2*, 519.
- (18) Cadot, O.; Bonn, D.; Douady, S. *Phys. Fluids* **1998**, *10*, 426.
- (19) Armstrong, R.; Jhon, M. S. *Chem. Eng. Commun.* **1984**, *30*, 99.
- (20) Berman, N. S. *Annu. Rev. Fluid Mech.* **1978**, *10*, 47.
- (21) Choi, H. J.; Kim, C. A.; Sohn, J. I.; Jhon, M. S. *Polym. Degrad. Stab.* **2000**, *69*, 341.
- (22) Zakin, J. L.; Hunston, D. L. *J. Appl. Polym. Sci.* **1978**, *22*, 1763.
- (23) Culter, J. D.; Zakin, J. L.; Patterson, G. K. *J. Appl. Polym. Sci.* **1975**, *19*, 3235.
- (24) Horn, A. F.; Merrill, E. W. *Nature (London)* **1984**, *312*, 140.
- (25) Rodriguez, F.; Winding, C. C. *Ind. Eng. Chem.* **1959**, *51*, 1281.
- (26) Moussa, T.; Tiu, C.; Sridhar, T. *J. Non-Newtonian Fluid Mech.* **1993**, *48*, 261.
- (27) Smith, D. E.; Babcock, H. P.; Chu, S. *Science* **1999**, *283*, 1724.
- (28) Babcock, H. P.; Smith, D. E.; Hur, J. S.; Shaqfeh, E. S. G.; Chu, S. *Phys. Rev. Lett.* **2000**, *85*, 2018.
- (29) Mason, T. G.; Dhople, A.; Wirtz, D. *Macromolecules* **1998**, *31*, 3600.
- (30) Zimm, B. H. *Macromolecules* **1998**, *31*, 6089.
- (31) Nguyen, T. T.; Shklovskii, B. I. *Phys. Rev. Lett.* **2002**, *89*, 018101.
- (32) Turner, S. W. P.; Cabodi, M.; Craighead, H. G. *Phys. Rev. Lett.* **2002**, *88*, 128103.
- (33) Kim, C. A.; Jo, D. S.; Choi, H. J.; Kim, C. B.; Jhon, M. S. *Polym. Testing* **2001**, *20*, 43.
- (34) Tong, P.; Goldburg, W. I.; Huang, J. S.; Witten, T. A. *Phys. Rev. Lett.* **1990**, *65*, 2780.
- (35) McCormick, C. L.; Hester, R. D.; Morgan, S. E.; Safieddine, A. M. *Macromolecules* **1990**, *23*, 2124.
- (36) McCormick, C. L.; Hester, R. D.; Morgan, S. E.; Safieddine, A. M. *Macromolecules* **1990**, *23*, 2132.
- (37) Lim, S. T.; Lee, K.; Kim, C. A.; Choi, H. J.; Kim, J. G.; Jhon, M. S. *J. Ind. Eng. Chem.* **2002**, *8*, 365.
- (38) Kim, C. A.; Sung, J. H.; Choi, H. J.; Kim, C. B.; Chun, W.; Jhon, M. S. *J. Chem. Eng. Jpn.* **1999**, *32*, 803.
- (39) Choi, H. J.; Kim, C. A.; Jhon, M. S. *Polymer* **1999**, *40*, 4527.
- (40) Yu, J. F. S.; Zakin, J. L.; Patterson, G. K. *J. Appl. Polym. Sci.* **1979**, *23*, 2493.
- (41) Sasaki, N.; Maki, Y.; Nakata, M. *J. Appl. Polym. Sci.* **2002**, *83*, 1357.
- (42) Odel, J. A.; Keller, A.; Miles, M. J. *Polym. Commun.* **1983**, *24*, 7.
- (43) Frenkel, J. *Acta Physicochim. URSS* **1994**, *19*, 51.
- (44) Odel, J. A.; Keller, A. *J. Polym. Sci., Polym. Phys.* **1986**, *24*, 1889.
- (45) Merrill, E. W.; Horn, A. F. *Polym. Commun.* **1984**, *25*, 144.
- (46) Sreenivasan, K. R.; Meneveau, C. *Phys. Rev. A* **1988**, *38*, 6287.
- (47) Brostow, W.; Ertepınar, H.; Singh, R. P. *Macromolecules* **1990**, *23*, 5109.

MA025964K